catalysts

Article

Preparation of di-[EMIM]$CoCl_3$ Ionic Liquid Catalyst and Coupling with Oxone for Desulfurization at Room Temperature

Shaokang Wang [1] and Hang Xu [1,2,*]

[1] School of Chemistry and Chemical Engineering, Henan University of Science and Technology, Luoyang 471023, China
[2] Provincial and Ministerial Co-Construction of Collaborative Innovation Center for Non-Ferrous Metal New Materials and Advanced Processing Technology, Luoyang 471023, China
* Correspondence: xhinbj@126.com

Abstract: The intermediate di-[EMIM]Cl was synthesized from methyl imidazole and 1,4-dichlorobutane and then reacted with cobalt chloride at 105 °C to prepare a bi-[EMIM]$CoCl_3$ ionic liquid catalyst. The di-[EMIM]$CoCl_3$ catalyst coupled with oxone to remove sulfur-containing organics in octane. The di-[EMIM]$CoCl_3$ catalyst was characterized by HNMR, FTIR, TG, and SEM–EDS. The dibenzothiophene (DBT) was dissolved in octane to prepare a model oil with an initial sulfur content of 500 ppm. Six grams of the model oil was added. The results showed that the optimal dosages of di-[EMIM]$CoCl_3$, oxone (20 wt%), and [BMIM]BF_4 extractant were 1 g, 2 g, and 2 g, respectively. At the optimum temperature of 45 °C, 100% of sulfur was removed after 40 min. After di-[EMIM]$CoCl_3$ was recycled five times, the sulfur removal percentage remained above 91%. The sulfur removal percentages for different sulfur-containing organics followed the order of dibenzothiophene (DBT) > benzothiophene (BT) > 4,6-dimethyldibenzothiophene (4,6-DMDBT). The oxidation product was determined to be $DBTO_2$ by GC–MS analysis, and the oxidation mechanism was discussed. The active oxygen atoms of oxone oxidized DBT to form DBTO, and then persulfate oxidized DBTO to $DBTO_2$ via an identical oxidation mechanism.

Keywords: dicationic ionic liquids; cobalt chloride; oxone; desulfurization; catalytic oxidation

Citation: Wang, S.; Xu, H. Preparation of di-[EMIM]$CoCl_3$ Ionic Liquid Catalyst and Coupling with Oxone for Desulfurization at Room Temperature. *Catalysts* **2023**, *13*, 410. https://doi.org/10.3390/catal13020410

Academic Editor: Hyun-Seog Roh

Received: 17 January 2023
Revised: 7 February 2023
Accepted: 8 February 2023
Published: 15 February 2023

1. Introduction

Fuel desulfurization is important for atmospheric protection because toxic sulfur oxides, especially sulfur dioxide, released during the combustion of sulfur-containing oil products can deteriorate the air quality and lead to other environmental problems [1]. Therefore, ultra-low-sulfur fuel processing is an important development direction for the petrochemical industry. Fuel desulfurization can be used in this industry to produce low-sulfur or even sulfur-free fuel, including hydrodesulfurization [2] and non-hydrodesulfurization [3]. Hydrodesulfurization requires harsh operating conditions and has poor performance in removing aromatic sulfides [4]. Therefore, non-hydrodesulfurization technologies, which have a high removal efficiency for aromatic sulfides, have attracted attention. Extraction and catalytic oxidative desulfurization (ECODS) has mild operating conditions, a high desulfurization efficiency, and a short reaction time [5].

The key to ECODS is the oxidant selection and catalyst preparation. The most commonly used oxidant is hydrogen peroxide [6], which is environmentally friendly, efficient, and moderately priced. However, it is unstable and rapidly loses its performance. By contrast, the physical property of oxone is solid powder. Oxone [7] is more stable, inexpensive, and can be more easily stored and transported, making it an ideal desulfurization oxidant. The drawback of persulfate is that it decomposes when the temperature is higher than 70 °C. The operating temperature of the ECODS process is generally room temperature or close to it and does not exceed 60 °C. Therefore, oxone was selected as the oxidant in this study. Catalysts can accelerate the oxidation desulfurization rate, so the design and preparation of high-efficiency catalysts, especially metal-containing ionic liquids, is another desulfurization research hotspot [8].

Metal-containing ionic liquids have structural designability, which makes them suitable for designing desulfurization catalysts. Chen XC et al. [9] synthesized a series of Lewis acid ionic liquid catalysts, i.e., $[C_4min]Cl/MCl_2$ (M = Zn, Fe, Cu, Mg, Sn, and Co), using 1-*n*-butyl-3-methylimidazole and multiple metal chlorides. The results showed that $[C_4mim]Cl/3ZnCl_2$ had the best desulfurization performance. Zhao RX et al. [10] mixed [HDMF]Cl with either iron chloride or zinc chloride to prepare $[HDMF]Cl/0.2FeCl_3$ and $[HDMF]Cl/ZnCl_2$. The experimental results showed that the removal percentages of dibenzothiophene (DBT) in the presence of the two catalysts were 98.08% and 99.2%, respectively. Alenazi B et al. [11] used four imidazole-based ionic liquid complexes containing different metal ions (Mn^{2+}, Fe^{2+}, Ni^{2+}, and Co^{2+}) and metal oxide-based nanomaterials as catalysts. The study indicated that all catalysts had excellent catalytic desulfurization performance. Li ET et al. [12] prepared magnetic imidazole ionic liquids (MIL) $[C_6min]Br/FeCl_3$ catalysts that contained alkanes with different numbers of carbon atoms by using $FeCl_3$. These catalysts displayed remarkable catalytic desulfurization performance. Zhang M et al. [13] used the imidazole cation and the polyoxometalate anion to prepare a vanadium-substituted polyoxometalate ionic liquid ($[C_4VIM]PMoV_2$) as a catalyst. The sulfur removal percentage reached 98.9% under optimal conditions. Xu H et al. [14] prepared a cobalt-containing ionic liquid ($[BMIM]CoCl_3$) loaded on silica gel as a catalyst, and the removal percentage of DBT in the presence of this catalyst reached 99.5%.

Double ionic liquids (di-ILs) are new ionic liquids that are composed of two single cationic liquids connected by an alkane or aromatic hydrocarbon [15]. Compared with single ionic liquids, double ionic liquids are more stable, with lower toxicity [16] and larger cations. A larger cation results in stronger π-π interactions between cations and aromatic sulfides, which are more conducive to the capture of sulfur-containing compounds [17]. Thus, the desulfurization efficiency is enhanced. In addition, through electrostatic interactions, the double cations are well-connected to the anions, which improves the overall activity of the catalyst [18]. The carbon chain between the two cations undergoes bending and stretching vibrations that can enhance their ability to capture and remove sulfur-containing compounds. Because of their unique properties, double ionic liquids have been successfully applied in catalytic desulfurization. Li et al. [19] prepared a double phosphotungstate ionic liquid catalyst, coupled it with hydrogen peroxide, and achieved a high desulfurization efficiency with it. Li et al. [17] prepared a double acidic ionic liquid as an extractant to investigate the extraction of DBT from fuel oil because increasing the volume of the cations increased the aromatic π-electron density of the cations and reduced the electrostatic force between the anions and cations so that the $\pi-\pi$ interaction between the cations and aromatic sulfides became larger, which made the extraction of aromatic sulfides from oil into ILs easier.

The cobalt ion and oxone together in aqueous exhibit an excellent oxidation ability and are widely used in organic wastewater treatment. In our previous study, a single cobalt ion was fixed in an ionic liquid to form a desulfurization ionic liquid [14] ($[BMIM]/CoCl_3$). The physical property of $[BMIM]/CoCl_3$ in the desulfurization process was a viscous liquid at room temperature. The drawback was the high price due to the large dosage. The solid technology of ionic liquids is a strategy to reduce the dosage. In this study, a new double cobalt-containing ionic liquid (di-$[EMIM]CoCl_3$) was prepared by the carbon chain connection of a single cobalt-containing ionic liquid catalyst. The double cobalt-containing ionic liquid expressed solid physical properties at room temperature, which could increase the density of cobalt ions in the catalyst and decrease the dosage of the catalyst. As it should be, the high price of functional ionic liquids is still the drawback of this study.

The di-$[EMIM]CoCl_3$ was characterized by HNMR, FTIR, TG, and SEM–EDS and coupled with oxone to form a desulfurization system to remove benzothiophene (BT), DBT, and 4,6-dimethyldibenzothiophene (4,6-DMDBT) from octane (stimulant fuel). $[BMIM]BF_4$ ionic liquid was selected as the desulfurization extractant because it could hardly dissolve with octane. The effects of the di-[EMIM]$CoCl_3$ dosage, oxone (20 wt%) dosage, [BMIM]BF_4 dosage, desulfurization temperature, and different sulfur organisms were discussed. The recycling performance of the catalyst was also studied. The desulfurization products were analyzed by GC–MS, and the desulfurization mechanism was discussed.

2. Experimental

2.1. Preparation of Ionic Liquid Catalyst

The preparation process of ionic liquid catalyst is shown in Figure 1. Acetonitrile (12 mL), 5 mL of methylimidazole, and 3.3 mL of 1,4-dichlorobutane were added to a three-necked flask with a condensation reflux device and a heating device. The reaction temperature was controlled at 80 °C for 24 h, and a white precipitate was obtained. After the precipitate was washed and purified several times by ethyl acetate, it was vacuum dried for 12 h, and then a white powder di-[EMIM]Cl ionic liquid was obtained [20]. The di-[EMIM]Cl powder was physically mixed with cobalt chloride in a molar ratio of 1:2, and the resulting mixture was placed in a blast drying oven for 24 h at 105 °C. Afterward, a blue di-[EMIM]$CoCl_3$ ionic liquid desulfurization catalyst was obtained. All the chemicals were analytical reagents purchased from Aladdin Reagent Company (Shanghai, China). All the chemicals were used without any purification. The water used in the experiment was deionized water.

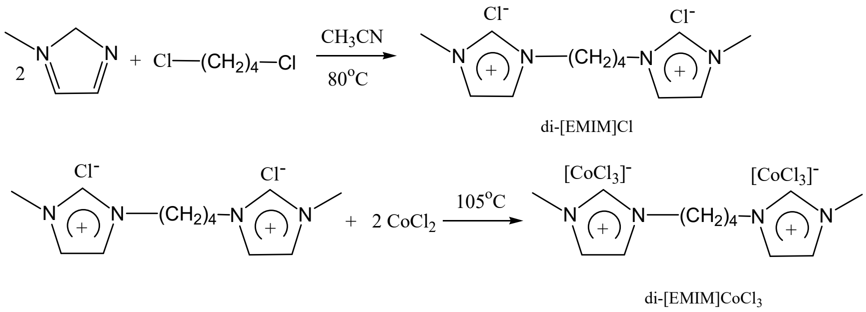

Figure 1. Synthesis process of di-[EMIM]$CoCl_3$.

2.2. Desulfurization Process

Dibenzothiophene (DBT) was dissolved in n-octane to obtain a simulated fuel with an initial sulfur content of 500 ppm. The method for preparing simulated fuel containing benzothiophene (BT) or 4,6-dimethyldibenzothiophene (4,6-DMDBT) was the same as that for preparing simulated DBT fuel. Then, 500 ppm DBT solution, di-[EMIM]$CoCl_3$ catalyst, and [BMIM]BF_4 extractant were added to a 50 mL round-bottom flask, and the extraction equilibrium was reached after magnetic stirring for 30 min. At the "0" time, oxone (20 wt%) was added, and the catalytic oxidization desulfurization reaction was started. The sulfur contents in the simulated fuel were sampled and analyzed at a certain interval. The analyzed method referred to Ref. [21], and the formula for calculating the desulfurization rate was as follows:

$$\mathrm{Sulfur Removel} = \frac{[\mathrm{S}]_0 - [\mathrm{S}]_t}{[\mathrm{S}]_0} \quad (1)$$

Here, "Sulfur Removal" represents the desulfurization rate, $[S]_0$ represents the initial sulfur content, and $[S]_t$ represents the sulfur content at time t.

2.3. Characterization

The thermogravimetric analysis (TGA) of di-[EMIM]$CoCl_3$ was performed on a TG-DTA8122 (Rigaku, Osaka, Japan) with a 40 mL min^{-1} air atmosphere and a 20 °C min^{-1} heating rate. The micromorphology of di-[EMIM]$CoCl_3$ was analyzed via scanning electron microscopy and energy-dispersive X-ray spectroscopy on FlexSEM 1000 (Hitachi, Tokyo, Japan). The infrared spectrum of di-[EMIM]$CoCl_3$ was carried out using a Trace 100 infrared spectrometer (Shimadzu, Kyoto, Japan). The HNMR of di-[EMIM]Cl was recorded on a Bruker ASCEND spectrometer. The product was analyzed by gas chromatography–mass spectrometry using a Finnigan Trace GC 2000 chromatograph equipped with an HP-1 capillary column (30 m × 0.32 mm i.d., 0.25 µm phase thickness) and Trace MS 2000 mass spectrometer (ThermoQuest Finnigan, Boston, MA, USA).

3. Results and Discussions

3.1. HNMR and FTIR of di-[EMIM]Cl

The HNMR data of di-[EMIM]Cl was as follows: ^{1}H NMR (400 MHz, D_2O-d_6, δ/ppm relative to TMS) for [EMIM]Cl: 1.83(2H, dt, CH_2), 3.82(3H, s, CH_3), 4.17(2H, t, CH_2), 7.39(1H, d, CH), 8.66(1H, s, CH), which indicated that pure di-[EMIM]Cl was synthesized.

The FTIR of di-[EMIM]Cl is shown in Figure 2. The intermediate, di-[EMIM]Cl ionic liquid, had a strong water absorption capacity. In Figure 2, the biggest infrared absorption peak (3200–3600 cm^{-1}) was attributed to the stretching vibration of hydrogen and oxygen bonds. There was an interesting experimental phenomenon in which cobalt chloride entered into the di-[EMIM]Cl ionic liquid to form di-[EMIM]$CoCl_3$, which had a worse water absorption capacity. Next, the peak at 3097 cm^{-1} was attributed to the C-H stretching vibration of the imidazole ring. The absorption peak at 2954 cm^{-1} verified the presence of CH_3 [22], which was in the imidazole ring. The peaks at 1622 cm^{-1} and 1574 cm^{-1} were attributed to the C=C and C=N vibrations of the imidazole ring skeleton. The peak at 1462 cm^{-1} was attributed to methylene (-CH_2-) groups [23], which comprised the carbon chain connecting the two imidazole rings. The peak at 1168 cm^{-1} was attributed to the C-N stretching vibration [24]. The peak at 621 cm^{-1} was attributed to the out-of-plane bending deformation of the imidazole ring [25]. This spectrum is consistent with that of di-[EMIM]Cl ionic liquid.

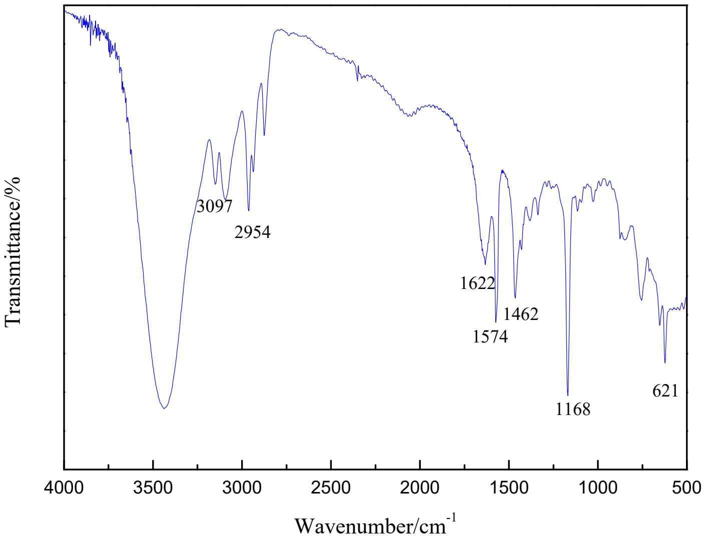

Figure 2. FTIR of di-[EMIM]Cl ionic liquid.

3.2. TG and SEM–EDS of di-[EMIM]$CoCl_3$

It can be seen in Figure 3 that the ionic liquid underwent three stages of weight loss. The first stage occurred below 283.9 °C, and its weight loss was only 3.40%, which mainly corresponded to the evaporation of water absorbed by the ionic liquid. The second stage occurred in the range of 283.9–477.4 °C, and the weight decreased by 61.68%, which corresponded to the decomposition and volatilization of the ionic liquid. The third weight loss stage (12.86%) occurred above 477.4 °C, which corresponded to the oxidation of cobalt chloride and the volatilization of chlorine. The oxidized product was Co_2O_3 according to the calculated residual weight. According to the analysis of the DTA curve, the whole experimental process was endothermic, and the ionic liquid underwent the fastest decomposition at 417.1 °C. Thermogravimetric analysis indicated that di-[EMIM]$CoCl_3$ had good thermal stability below 283.9 °C. In addition, di-[EMIM]$CoCl_3$ began to melt when the temperature was raised above 90 °C, so it was solid at the operating temperature of the desulfurization experiment.

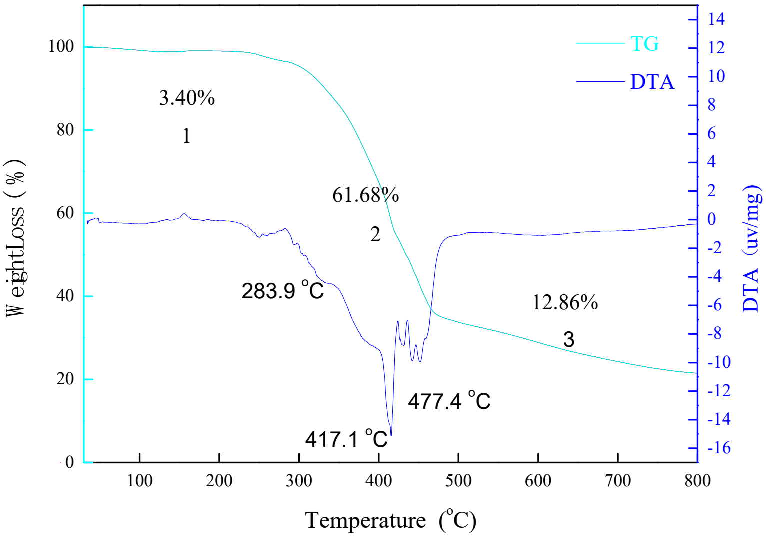

Figure 3. TG analysis of di-[EMIM]$CoCl_3$.

It can be seen from the ionic liquid morphology in Figure 4a,b that di-[EMIM]Cl and $CoCl_2$ completely fused to form di-[EMIM]$CoCl_3$. After agglomeration, the particles were larger and had an irregular morphology. The surface of the particles was very rough with many small pores. It can be seen in the EDS maps in Figure 4c that the ionic liquid was composed of C, N, Cl, and Co elements, where the Co atoms were evenly distributed on the outer surface of the catalyst. Such a microscopic surface and distribution of catalytically active Co species were conducive to reactant adsorption, surface reactions, and product removal. According to the EDS results in Figure 4d,e, the mass proportions of C, N, Cl, and Co were 28.26%, 12.34%, 38.02%, and 21.34%, respectively, and their atomic proportions were 54.91%, 15.86%, 21.23%, and 7.99% respectively. According to the molecular structure of di-[EMIM]$CoCl_3$, the theoretical mass proportions of C, N, Cl, and Co were 26%, 10%, 38%, and 21%, respectively, and their theoretical atomic proportions were 50%, 16%, 26%, and 8%, respectively. The theoretical values were similar to the EDS values, which verified the successful preparation of pure di-[EMIM]$CoCl_3$ ionic liquid.

3.3. *Effect of di-[EMIM]$CoCl_3$ Dosage*

DBT-containing simulated oil (6 g) with an initial sulfur content of 500 ppm was taken. [BMIM]BF_4 (1 g) was taken as an extractant, and 1 g of oxone solution (20 wt%) was added. The reaction temperature was controlled at 45 °C. The changes in the sulfur removal percentage over time under different dosages of di-[EMIM]$CoCl_3$ ionic liquid are shown in Figure 5. The period from −30 min to 0 min was attributed to the extraction stage (the first stage), and the sulfur removal percentages were 17.2%, 19.1%, 21.9%, 23.5%, and 26.6%, which respectively corresponded to 0.5 g, 0.75 g, 1 g, 1.25 g, and 1.5 g of di-[EMIM]$CoCl_3$ ionic liquid added. Without the catalyst, only [Bmim]BF_4 extractant showed 15.4% sulfur removal after the 30 min extraction process. The results indicated that DBT in the octane phase could be extracted by the ionic liquid and [BMIM]BF_4. The extracted percentage of DBT in the first stage increased slightly upon increasing the catalyst dosage, which also verified that the transfer of DBT from the oil phase to the reaction phase mainly depended on its extraction by [BMIM]BF_4. The di-[EMIM]$CoCl_3$ ionic liquid had a stronger adsorption capability for DBT. The adsorption sulfur removal percentage when using 1 g of di-[EMIM]$CoCl_3$ ionic liquid was about 9%, and the extraction's sulfur removal percentage of pure [BMIM]BF_4 was about 13%. The period from 0 min to 60 min was attributed to the catalytic oxidation desulfurization stage (the second stage). After adding oxone as an oxidant, the desulfurization process accelerated significantly. The catalytic activity of di-[EMIM]$CoCl_3$ was displayed in the second stage. At 60 min, di-[EMIM]$CoCl_3$ dosages of 0.5 g, 0.75 g, 1 g, 1.25 g, and 1.5 g corresponded to sulfur removal percentages of 50.65%, 62.62%, 80.1%, 80.3%, and 75.7%, respectively. The desulfurization results indicated that upon increasing the dosage of di-[EMIM]$CoCl_3$, the sulfur removal percentage increased first and then decreased. The sulfur removal percentage reached the maximum when the dosages were 1 g and 1.25 g. The period after 60 min was attributed to the final stage of desulfurization (the third stage), after which the desulfurization reaction did not occur. The sulfur removal percentage was related to the desulfurization mechanism. The divalent cobalt ions of the ionic liquid could interact with the oxone oxidant to form a Fenton-like system and generate trivalent cobalt ions and sulfate radicals [26] that could oxidize DBT. However, excess divalent cobalt ions reacted with sulfate radicals and generated sulfate ions [27], which decreased the sulfur removal percentage due to oxidation. Chloride ions could also react with sulfate radicals, which may have inhibited the final desulfurization efficiency [28]. Therefore, there was an optimum catalyst dosage corresponding to the specific oxidant level. In this study, the optimum catalyst dosage was 1.0 g, and the corresponding sulfur removal percentage reached 80.1%.

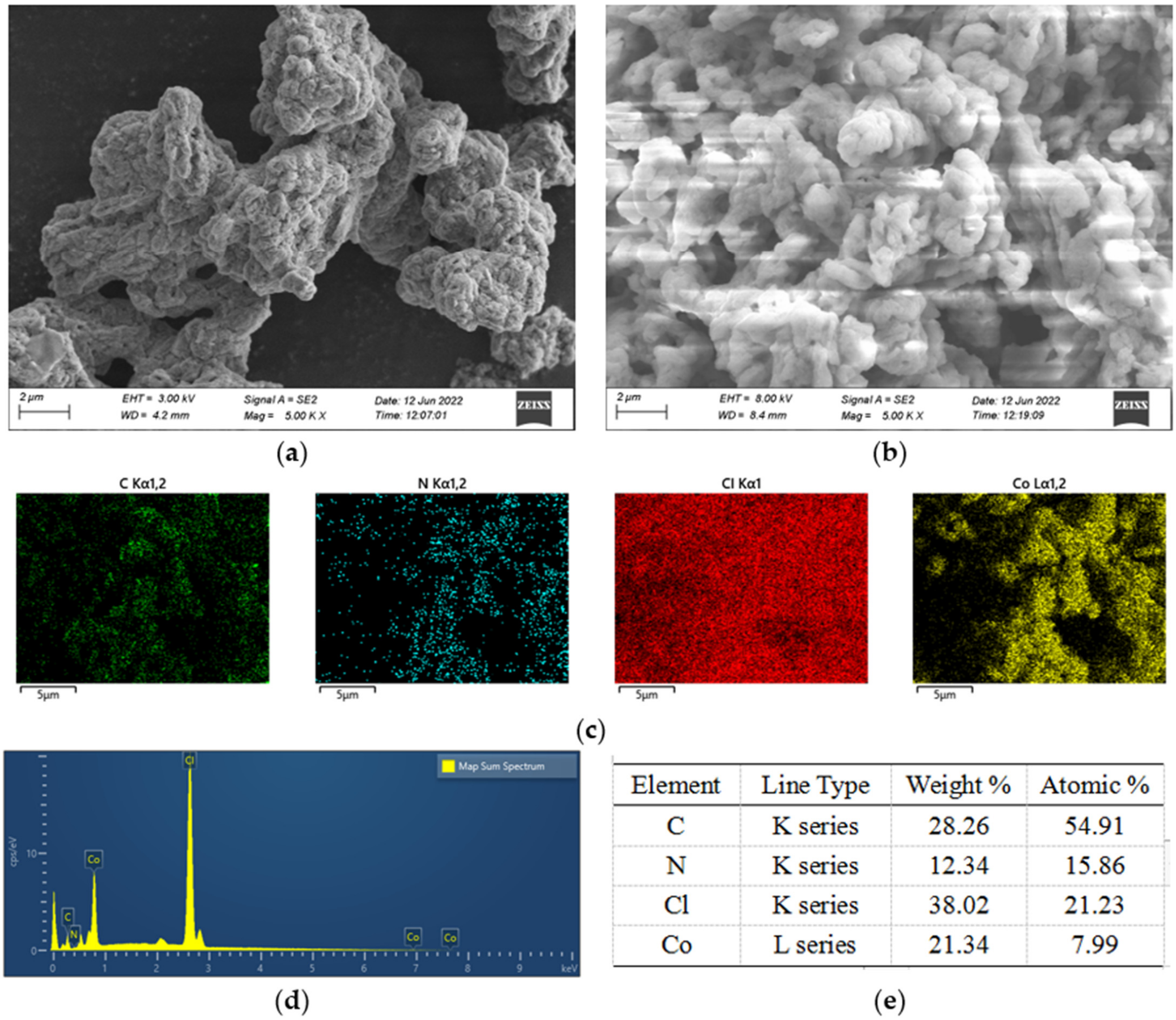

(a) (b)

(c)

(d) (e)

Element	Line Type	Weight %	Atomic %
C	K series	28.26	54.91
N	K series	12.34	15.86
Cl	K series	38.02	21.23
Co	L series	21.34	7.99

Figure 4. (**a**,**b**) SEM, (**c**) mapping imagesand, (**d**,**e**) EDS of di-[EMIM]$CoCl_3$.

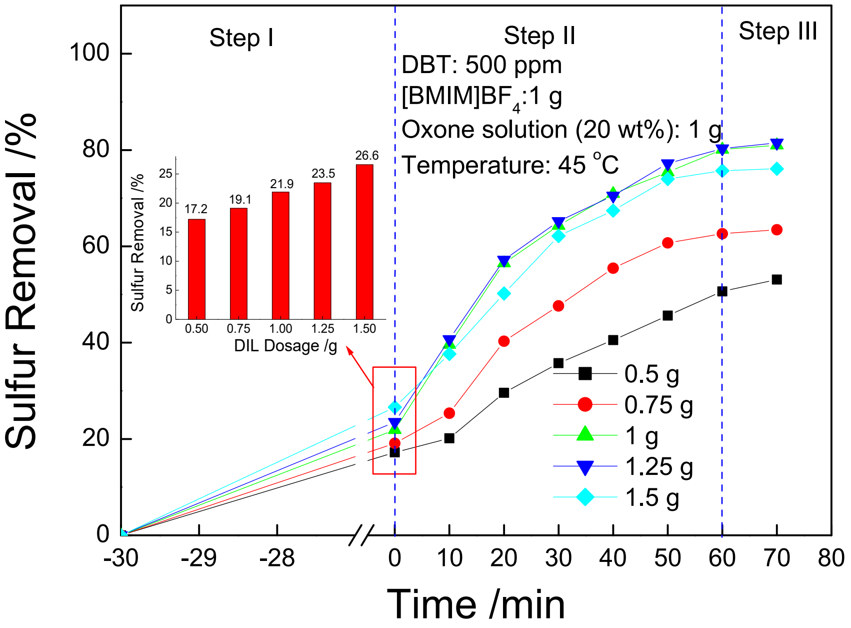

Figure 5. Effect of di-[EMIM]$CoCl_3$ dosage.

3.4. Effect of Oxone (20wt%) Dosage

It can be seen in Figure 6 that the sulfur removal percentage in the first stage (extraction stage) was about 21%. When the oxone oxidant (20 wt%) was added, the catalytic oxidation process (the second stage) began. The sulfur removal percentage rose rapidly upon increasing the oxidant dosage. When oxone (20 wt%) increased to above 2 g, the sulfur removal percentage began to decrease. After 60 min, oxone (20 wt%) dosages of 0.50 g, 1.00 g, 1.50 g, 2.00 g, and 2.50 g resulted in sulfur removal percentages of 66%, 80%, 92%, 100%, and 96%, respectively. When the reaction time exceeded 60 min, almost no desulfurization occurred, indicating that the third stage (desulfurization ends) had begun. The experimental results showed that the optimal oxidant dosage was 2 g under the experimental conditions. The oxone oxidant was the direct source of peroxydisulfate radicals, so increasing the oxone dosage significantly increased the sulfate radical concentration. However, there was an optimal oxidant-to-sulfur concentration ratio and an optimal oxidant-to-catalyst concentration ratio. When oxone was in excess, sulfate radicals were also quenched [29,30], which decreased the sulfur removal percentage. During catalytic oxidative desulfurization, the oxidant concentration should be present in slight excess. However, when oxone was in excess, the catalyst could not fully catalyze the oxidant, preventing it from exerting its maximum efficiency and causing waste. Therefore, the oxone (20 wt%) dosage was set to 2 g in the following experiments.

3.5. Effect of [BMIM]BF_4 Dosage

It can be seen in Figure 7 that during the extraction stage, the extraction sulfur removal percentage increased from 9.7% to 45.2% when the [BMIM]BF_4 dosage increased from 0 g to 2.5 g. The extraction percentage was 9.7% in the absence of [BMIM]BF_4 because di-[EMIM]$CoCl_3$ could adsorb DBT. After entering the catalytic oxidation desulfurization stage, the sulfur removal percentage increased rapidly and different extractant dosages, resulting in different desulfurization efficiencies. When the extractant dosage increased from 0 g to 2 g, the sulfur removal percentage increased upon increasing the extraction percentage. When it further increased to 2.5 g, the sulfur removal percentage began to decrease. When the optimal extractant dosage was kept at 2 g, a 40 min catalytic oxidation removed 100% of the sulfur, which resulted in a 20 min faster complete desulfurization compared with that when the extractant dosage was 1 g. During desulfurization, an appropriate catalyst concentration and oxidant concentration need to be maintained to achieve the best desulfurization efficiency. [BMIM]BF_4 acted not only as an extractant but also as a reaction medium. When [BMIM]BF_4 acted as the reaction medium, a lower dosage increased the concentration of both the catalyst and the oxidant. Therefore, although 2.5 g [BMIM]BF_4 led to the highest extraction efficiency, the corresponding catalyst and oxidant concentrations may have been relatively low and not conducive to the subsequent catalytic oxidation reaction. Only a 56% sulfur removal percentage was achieved within 40 min when using 0.5 g [BMIM]BF_4 because this dosage resulted in excessively high catalyst and oxidant concentrations. This intensified the quenching reaction and inhibited the desulfurization process.

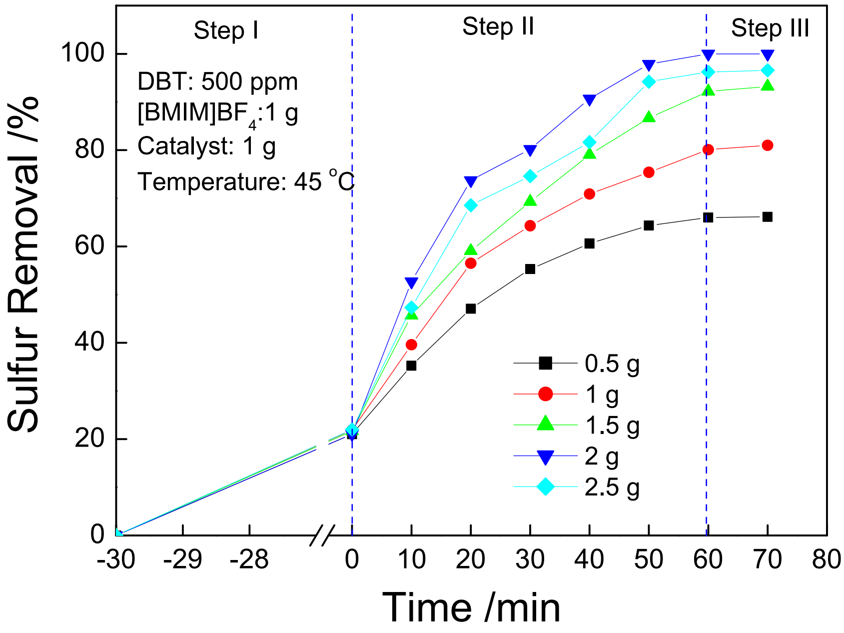

Figure 6. Effect of oxone (20 wt%) dosage.

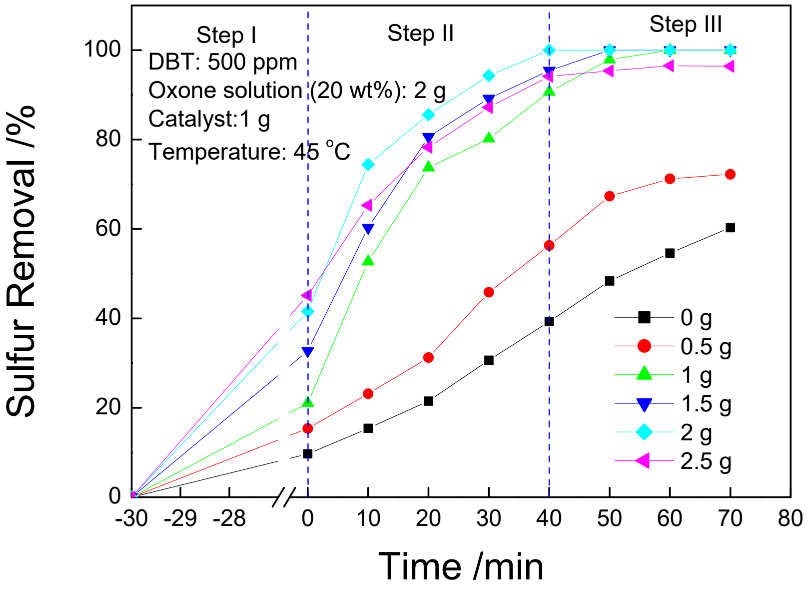

Figure 7. Effect of [BMIM]BF_4 dosage.

3.6. Effect of Temperature

Figure 8 shows that during the extraction stage, the extraction sulfur removal percentage slightly increased with the temperature. Specifically, the extraction sulfur removal percentages were 40.5%, 41.5%, and 43.3% at 30 °C, 45 °C, and 60 °C, respectively. The viscosity of the ionic liquid decreased and the extraction percentage slightly increased upon increasing the temperature. During the reaction phase (0–40 min), the sulfur removal percentage varied with the temperature as follows: 45 °C > 30 °C > 60 °C. When the temperature was 30 °C, the viscosities of [BMIM]BF_4 extractant and [EMIM]$CoCl_3$ catalyst were relatively high and were not conducive to the thermal motion of molecules. Accordingly, the ability of cobalt ions to catalytically activate peroxydisulfate at 30 °C was also low. Therefore, the sulfur removal percentage at 30 °C was about 8% lower than that at 45 °C. When the temperature was 60 °C, the viscosity of the ionic liquid decreased, which was conducive to the thermal motion of molecules. However, at 60 °C, the oxidation capability of the oxidant peroxydisulfate was worse due to its easy decomposition, which caused it to rapidly lose its performance. Therefore, the sulfur removal percentage at 60 °C was about 20% lower than that at 45 °C. After 40 min, the desulfurization process was basically completed [31,32].

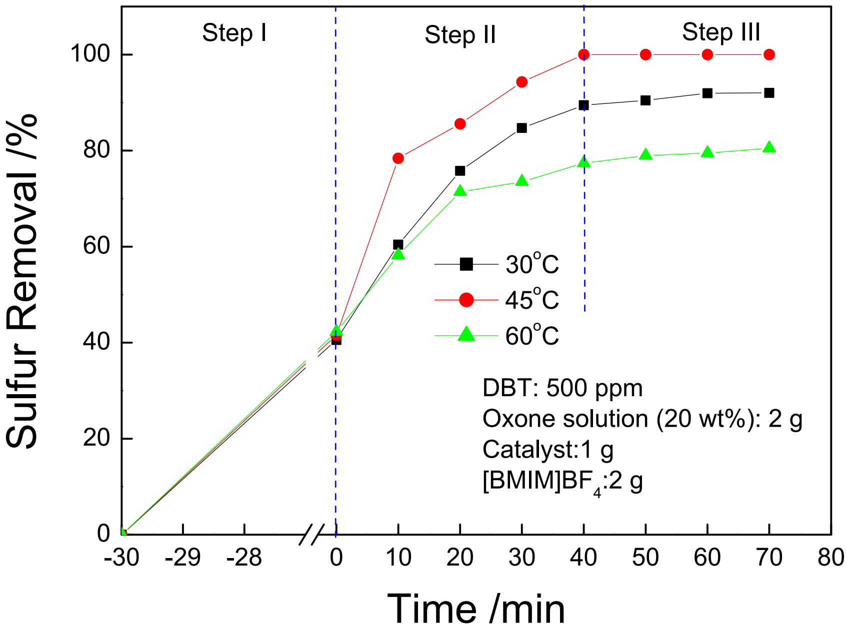

Figure 8. Effect of temperature.

3.7. Effect of Different Sulfur Organic Compounds

It can be seen in Figure 9 that during the first stage, the order of sulfur removal percentage of the three sulfur-containing compounds by [BMIM]BF_4 was DBT > BT > 4,6-DMDBT. In the second stage, the sulfur removal percentage of DBT reached 100% after 40 min, while the sulfur removal percentages of BT and 4,6-DMDBT were 64% and 61%, respectively, at this time. Their reaction endpoints were not reached. After 60 min, the reaction ended for BT and 4,6-DMDBT, and the sulfur removal percentages of the two were 82.01% and 76.03%, respectively. This shows that the sulfur removal percentages for different sulfur-containing organic matter followed the order of DBT > BT > 4,6-DMDBT. The electron cloud densities of the sulfur atoms of BT were lower than those of DBT and 4,6-DMDBT [33,34], so the sulfur atoms of BT were less active and more difficult to oxidize. The two methyl groups of the imidazole ring in 4,6-DMDBT have steric hindrance, which made the sulfur atoms difficult to oxidize.

3.8. Recycling Performance of di-[EMIM]$CoCl_3$

The recycling performance of a catalyst is important for potential industrial applications. After the desulfurization process, the reaction solvent ([BMIM]BF_4) was a hydrophobic ionic liquid, which was easily separated from the fuel owing to its very low mutual miscibility. The recycled di-[EMIM]$CoCl_3$/[BMIM]BF_4 mixture was heated at 120 °C for 6 h in order to decompose oxone and remove H_2O. The recycled di-[EMIM]$CoCl_3$/[BMIM]BF_4 mixture was used in a subsequent desulfurization cycle of a model fuel under similar conditions. It can be seen in Figure 10 that the sulfur removal percentage remained above 96% in the first four desulfurization stages, while it decreased to 91% in the fifth stage and 82% in the sixth stage. These results indicated that the catalytic system had a good recycling capacity. The reason for the deactivation of the catalytic system was the accumulation of sulfate and the oxidation products of DBT.

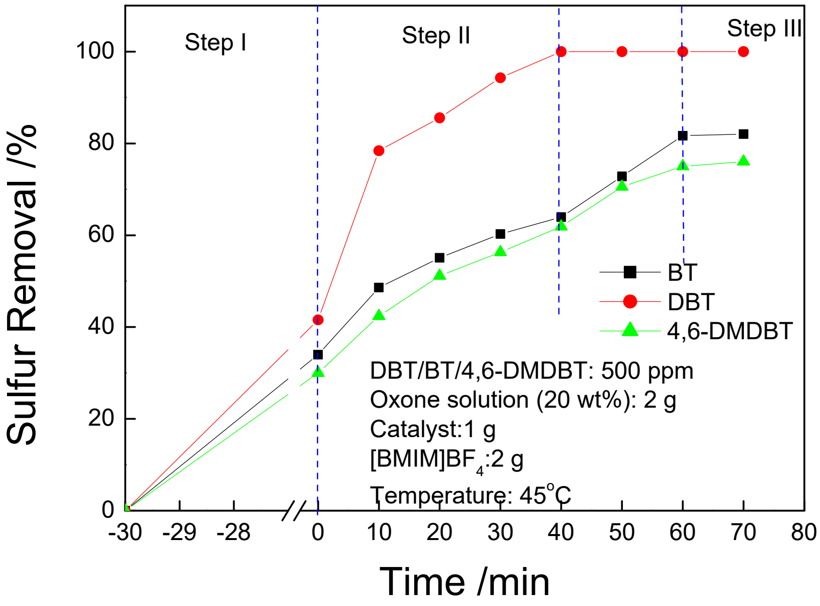

Figure 9. Effect of different sulfur organic compounds.

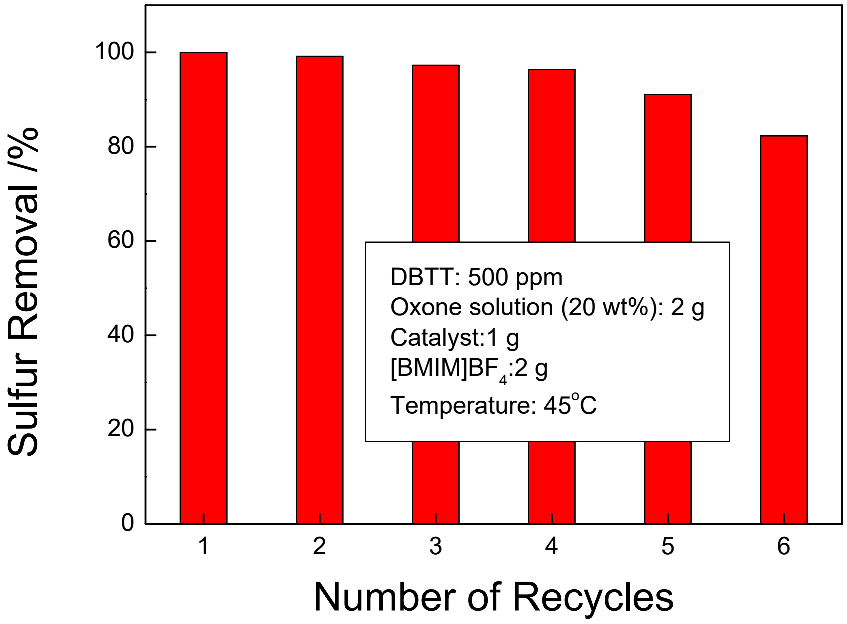

Figure 10. The recycling performance of di-[EMIM]$CoCl_3$.

3.9. Desulfurization Mechanism

GC–MS analysis showed that the oxidation product was $DBTO_2$, as shown in Figure 11a. The schematic diagram of the desulfurization mechanism is shown in Figure 11b. These results were used to propose a possible desulfurization mechanism. Step 1: under the effect of Co^{2+}, the O-O bond of hydrogen persulfate broke and formed hydroxyl radicals and sulfate radicals. During the breakage, Co^{2+} donated one electron to a hydroxyl radical and then formed Co^{3+} and OH^-. The sulfate radical was affected by the lone electron pair of the sulfur atom in BDT to form an S-O bond. Step 2: the S-O bond of the sulfate radical broke and formed a mono-oxygen dibenzothiophene sulfoxide (DBTO) and sulfite radical. Co^{3+} was unstable, so it could extract one electron from OH^- and return to Co^{2+}. The sulfite radical quenched the hydroxyl free radical to generate hydrogen sulfate. The entire process can be simplified as follows: the active oxygen atoms of persulfate oxidized DBT to form DBTO, and then persulfate oxidized DBTO to $DBTO_2$ via an identical oxidation mechanism [35].

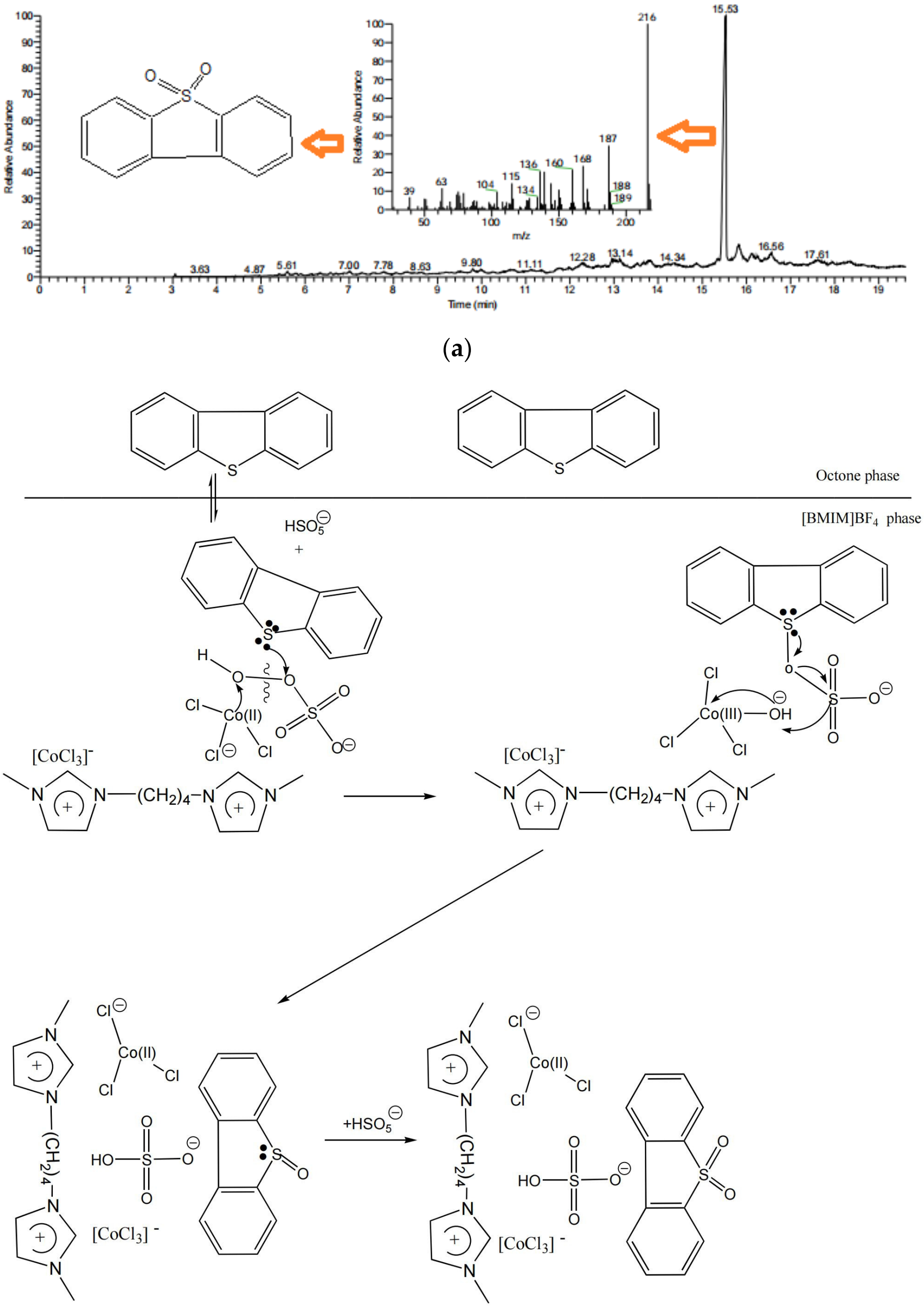

(a)

(b)

Figure 11. (**a**) GC–MS analysis and (**b**) desulfurization mechanism.

4. Conclusions

The di-[EMIM]$CoCl_3$ ionic liquid desulfurization catalyst was prepared and coupled with persulfate to carry out room-temperature desulfurization. DBT was dissolved in octane to prepare a model oil with an initial sulfur content of 500 ppm. Six grams of the model oil was added. The optimal dosages of di-[EMIM]$CoCl_3$, oxone (20 wt%), and [[BMIM]BF_4 extractant were 1 g, 2 g, and 2 g, respectively. At the optimum temperature of 45 °C, 100% of sulfur was removed after 40 min. After di-[EMIM]$CoCl_3$ was recycled five times, the sulfur removal percentage remained above 91%. The sulfur removal percentages for different sulfur-containing organics followed the order of DBT > BT > 4,6-DMDBT. The oxidation product was determined to be $DBTO_2$ by GC–MS analysis, and the oxidation mechanism was discussed. The active oxygen atoms of oxone oxidized DBT to form DBTO, and then persulfate oxidized DBTO to $DBTO_2$ via an identical oxidation mechanism.

Author Contributions: Experiment (synthesis and desulfurization), analysis (material and sulfur), writing, S.W.; conceptualization, writing and editing, reagents, equipment and supervision, H.X. All authors have read and agreed to the published version of the manuscript.

Funding: This research was funded by Nature Science Foundation of Henan Province, No: 202300410155.

Data Availability Statement: The data that support the findings of this study are available from the corresponding author, Hang Xu, upon reasonable request.

Conflicts of Interest: The authors declare no conflict of interest.

References

1. Lu, X.; Zhang, S.; Xing, J.; Wang, Y.; Chen, W.; Ding, D.; Wu, Y.; Wang, S.; Duan, L.; Hao, J. Progress of Air Pollution Control in China and Its Challenges and Opportunities in the Ecological Civilization Era. *Engineering* **2020**, *6*, 1423–1431. [CrossRef]
2. Saha, B.; Vedachalam, S.; Dalai, A.K. Review on recent advances in adsorptive desulfurization. *Fuel Process. Technol.* **2021**, *214*, 106685. [CrossRef]
3. Rajendran, A.; Cui, T.-Y.; Fan, H.-X.; Yang, Z.-F.; Feng, J.; Li, W.-Y. A comprehensive review on oxidative desulfurization catalysts targeting clean energy and environment. *J. Mater. Chem. A* **2020**, *8*, 2246–2285. [CrossRef]
4. Zhang, X.; Zheng, Y.; Chen, J.; Xue, H.; Liu, Y. A combined experimental and DFT study on the catalysis performance of a Co-doped MoS_2 monolayer for hydrodesulfurization reaction. *New J. Chem.* **2022**, *46*, 5065–5077. [CrossRef]
5. Xu, H.; Zhang, D.; Wu, F.; Wei, X.; Zhang, J. Deep desulfurization of fuels with cobalt chloride-choline chloride/polyethylene glycol metal deep eutectic solvents. *Fuel* **2018**, *225*, 104–110. [CrossRef]
6. Taghiyar, H.; Yadollahi, B. Keggin polyoxometalates encapsulated in molybdenum-iron-type Keplerate nanoball as efficient and cost-effective catalysts in the oxidative desulfurization of sulfides. *Sci. Total Environ.* **2020**, *708*, 134860. [CrossRef]
7. Xu, H.; Zhang, D.; Wu, F. Deep oxidative desulfurization of fuels based on [C_4mimCl]$CoCl_2$ ionic liquid oxone solutions at room temperature. *Fuel* **2017**, *208*, 508–513. [CrossRef]
8. Liu, F.; Yu, J.; Qazi, A.B.; Zhang, L.; Liu, X. Metal-Based Ionic Liquids in Oxidative Desulfurization: A Critical Review. *Environ. Sci. Technol.* **2021**, *55*, 1419–1435. [CrossRef]
9. Chen, X.; Song, D.; Asumana, C.; Yu, G. Deep oxidative desulfurization of diesel fuels by Lewis acidic ionic liquids based on 1-n-butyl-3-methylimidazolium metal chloride. *J. Mol. Catal. A Chem.* **2012**, *359*, 8–13. [CrossRef]
10. Zhao, R.-X.; Li, X.-P.; Mao, C.-F.; Hou, L.; Gao, X. [HDMF]Cl-based DES as highly efficient extractants and catalysts for oxidative desulfurization of model oil. *RSC Adv.* **2019**, *9*, 14400–14406. [CrossRef]
11. Alenazi, B.; Alsalme, A.; Alshammari, S.G.; Khan, R.A.; Siddiqui, M.R.H. Ionothermal Synthesis of Metal Oxide-Based Nanocatalysts and Their Application towards the Oxidative Desulfurization of Dibenzothiophene. *J. Chem.* **2020**, *2020*, 3894804. [CrossRef]
12. Li, E.; Zhu, Y.; Xu, Y. Desulfurization of gasoline by [$C_{4,\,6,\,8}$mim]Br/$FeCl_3$ ILs collaboration with CTAB. *Sep. Sci. Technol.* **2021**, *56*, 310–321. [CrossRef]
13. Zhang, M.; Liu, J.; Li, H.; Wei, Y.; Fu, Y.; Liao, W.; Zhu, L.; Chen, G.; Zhu, W.; Li, H. Tuning the electrophilicity of vanadium-substituted polyoxometalate based ionic liquids for high-efficiency aerobic oxidative desulfurization. *Appl. Catal. B Environ.* **2020**, *271*, 118936. [CrossRef]
14. Xu, H.; Zhang, J.; Zhang, D. Catalytic oxidation desulfurization of silica-gel-supported ionic liquid [Bmim]$CoCl_3$ coupling oxone. *Fuel* **2021**, *288*, 119655. [CrossRef]
15. Jiang, Y.; Wang, Z.; Xu, P. Dicationic Ionic Liquid @MIL-101 for the Cycloaddition of CO_2 and Epoxides under Cocatalyst-free Conditions. *Cryst. Growth Des.* **2021**, *21*, 3689–3698. [CrossRef]
16. Pérez, S.; Montalbán, M.; Carissimi, G.; Licence, P.; Víllora, G. In vitro cytotoxicity assessment of monocationic and dicationic pyridinium-based ionic liquids on HeLa, MCF-7, BGM and EA.hy926 cell lines. *J. Hazard. Mater.* **2020**, *385*, 121513. [CrossRef]

17. Li, J.; Lei, X.-J.; Tang, X.-D.; Zhang, X.-P.; Wang, Z.-Y.; Jiao, S. Acid Dicationic Ionic Liquids as Extractants for Extractive Desulfurization. *Energy Fuels* **2019**, *33*, 4079–4088. [CrossRef]
18. Verma, K.; Sharma, A.; Singh, J.; Badru, R. Ionic liquid mediated carbonylation of amines: Selective carbamate synthesis. *Sustain. Chem. Pharm.* **2021**, *20*, 100377. [CrossRef]
19. Li, J.; Guo, Y.; Tan, J. Polyoxometalate dicationic ionic liquids as catalyst for extractive coupled catalytic oxidative desulfurization. *Catalysts* **2021**, *11*, 356–362. [CrossRef]
20. Nezampour, F.; Ghiaci, M.; Farrokhpour, H. Dicationic ionic liquids/heteropoly acid composites as heterogeneous catalysts for cyclohexene oxidation with molecular oxygen under solvent-free condition: Insights from theory and experiments. *Appl. Catal. A-Gen.* **2017**, *543*, 104–114. [CrossRef]
21. Xu, H.; Wang, S.; Wu, F.; Yuan, Q.; Guo, Y.; Zhang, Y.; Wei, X.; Zhang, J. A fully-organic polymerization carrier calix[4]resorcinarene supported cobalt ionic liquid catalyst with oxone for desulfurization. *Fuel* **2022**, *318*, 123670. [CrossRef]
22. Barman, B.; Rajbanshi, B.; Yasmin, A. Exploring inclusion complexes of ionic liquids with alpha- and beta-cyclodextrin by NMR, IR, Mass, Density, Viscosity, Surface Tension and Conductance Study. *J. Mol. Struct.* **2018**, *1159*, 205–215. [CrossRef]
23. Wang, F.; Zhang, Z.; Yang, J.; Wang, L.; Lin, Y.; Wei, Y. Immobilization of room temperature Ionic Liquid (RTIL) on silica gel for adsorption removal of thiophenic sulfur compounds from fuel. *Fuel* **2013**, *107*, 394–399. [CrossRef]
24. Lin, Y.; Wang, F.; Zhang, Z. Polymer-supported ionic liquids: Synthesis, characterization and application in fuel desulfurization. *Fuel* **2014**, *116*, 273–280. [CrossRef]
25. Soliman, S.; Sanad, M.; Shalan, A. Synthesis, characterization and antimicrobial activity applications of grafted copolymer alginate-g-poly(N-Vinyl Imidazole). *RSC Adv.* **2021**, *11*, 11541–11548. [CrossRef] [PubMed]
26. Peng, Y.; Tong, W.; Xie, Y.; Hu, W.; Li, Y.; Zhang, Y.; Wang, Y. Yeast biomass-Induced Co_2p/biochar composite for sulfonamide antibiotics degradation through peroxymonosulfate activation. *Environ. Pollut.* **2021**, *268*, 115930. [CrossRef] [PubMed]
27. Ji, Y.; Dong, C.; Kong, D.; Lu, J. New insights into atrazine degradation by cobalt catalyzed peroxymonosulfate oxidation: Kinetics, reaction products and transformation mechanisms. *J. Hazard. Mater.* **2015**, *285*, 491–500. [CrossRef]
28. Zhu, J.; Li, H.; Shan, C.; Wang, S.; Lv, L.; Pan, B. Trace Co^{2+} coupled with phosphate triggers efficient peroxymonosulfate activation for organic degradation. *J. Hazard. Mater.* **2021**, *409*, 124920. [CrossRef]
29. Yan, S.; Geng, J.; Guo, R. Hydronium jarosite activation of peroxymonosulfate for theoxidation of organic contaminant in an electrochemical reactor driven by microbial fuel Cell. *J. Hazard. Mater.* **2017**, *333*, 358–368. [CrossRef]
30. Jia, J.; Liu, D.; Wang, S.; Li, H.; Ni, J.; Li, X.; Tian, J.; Wang, Q. Visible-light-induced activation of peroxymonosulfate by TiO_2 nano-tubes arrays for enhanced degradation of bisphenol. *Sep. Purif. Technol.* **2020**, *253*, 117510. [CrossRef]
31. Xiao, M.; Liu, H.; Gao, H.; Olson, W.; Liang, Z. CO_2 capture with hybrid absorbents of low viscosity imidazolium-based ionic liquids and amine. *Appl. Energy* **2019**, *235*, 311–319. [CrossRef]
32. Sadanandhan, A.M.; Khatri, P.K.; Jain, S.L. A novel series of cyclophosphazene derivatives containing imidazolium ionic liquids with variable alkyl groups and their physicochemical properties. *J. Mol. Liq.* **2019**, *295*, 111722. [CrossRef]
33. Liu, X.; Li, X.; Zhao, R. A facile sol-gel method based on urea-$SnCl_2$ deep eutectic solvents for the synthesis of SnO_2/SiO_2 with high oxidation desulfurization activity. *New J. Chem.* **2021**, *45*, 15901–15911. [CrossRef]
34. Cui, J.; Wang, G.; Liu, W.; Ke, P.; Tian, Q.; Li, X.; Tian, Y. Synthesis $BiVO_4$ modified by CuO supported onto bentonite for molecular oxygen photocatalytic oxidative desulfurization of fuel under visible light. *Fuel* **2021**, *290*, 120066. [CrossRef]
35. Hao, Y.; Ren, J. Extractive/catalytic oxidative mechanisms over $[Hnmp]Cl{\cdot}xFeCl_3$ ionic liquids towards the desulfurization of model oils. *New J. Chem.* **2019**, *43*, 7725–7732. [CrossRef]